

Timothy P. Dabbs,¹ Carolyn J. Fairbanks,² and
Brian R. Lawn²

Subthreshold Indentation Flaws in the Study of Fatigue Properties of Ultrahigh-Strength Glass

REFERENCE: Dabbs, T. P., Fairbanks, C. J., and Lawn, B. R., "Subthreshold Indentation Flaws in the Study of Fatigue Properties of Ultrahigh-Strength Glass," *Methods for Assessing the Structural Reliability of Brittle Materials, ASTM STP 844*, S. W. Freiman and C. M. Hudson, Eds., American Society for Testing and Materials, Philadelphia, 1984, pp. 142-153.

ABSTRACT: The rate-dependent characteristics of subthreshold indentation flaws in glass are surveyed. In the first part, the kinetics of radial crack initiation within the indentation field are described. It is shown that an incubation time must be exceeded in the contact process for a critical crack nucleus to develop. This incubation time decreases as the contact load and the water content in the environment increase. Even if incubation is not achieved *during* the contact, delayed pop-in may occur *after* the contact due to the action of residual stresses. Scanning electron microscopic evidence shows that the radial cracks initiate from precursor shear faults within the deformation zone. In the second part of the presentation, the fatigue properties of specimens with indentation flaws on either side of the threshold are discussed. The subthreshold flaws differ significantly from their postthreshold counterparts in these properties: the applied stresses at failure are higher, the susceptibility to water is stronger, and the scatter in individual data points is wider. These features are discussed in relation to the preceding crack-initiation kinetics. Finally, the implications of the results concerning design criteria for optical fibers are considered.

KEY WORDS: brittle materials, crack initiation, fatigue, glass, indentation flaw, optical fibers, radial crack, shear fault, strength, structural reliability

In an earlier paper in this volume [1] a strong argument was presented for the use of indentation flaws in the investigation of intrinsic fracture param-

¹Graduate student, School of Physics, University of New South Wales, New South Wales, Australia.

²Guest student and physicist, respectively, Center for Materials Science, National Bureau of Standards, Washington, D.C. 20234.

ters and flaw characteristics. One major advantage cited was the facility to control the scale of the flaw, by means of the contact load, in order to check for size effects in macroscopically determined crack growth laws. Such size effects would be apparent as deviations from the proposed "universal" plotting schemes. In view of the growing concern that microscopic flaws might differ in some significant respects from true cracks [2,3], particularly in the region of ultrahigh strengths (that is, approaching the theoretical limit), there would appear to be a need for systematic studies of flaw response at a fundamental level.

Accordingly, we survey here the results of some recent Vickers indentation studies on glass [4-6]. The original driving force for this work came from a pilot study on optical fibers [7] in which it was found that the strengths of specimens with indentations abruptly increased as the contact load diminished below some threshold. This threshold corresponded to a critical flaw configuration for crack *initiation*; the "pop-in" of radial cracks from the impression corners appeared to require the development of a sufficiently large precursor deformation zone [8,9]. Nevertheless, even though the subthreshold indentations were free of visible cracks, they still provided preferred sites for failure. It was therefore clear that the *mechanics*, if not the *mechanisms*, of failure were different at the subthreshold level. Thus, insofar as indentation flaws could be expected to simulate the broad features of certain natural flaw types in glass fibers, the conclusion could be drawn that extrapolations from macroscopic to microscopic domains, as is implicit in most (statistically based) strength analyses, may well be unjustified. Reported observations that the apparent crack velocity exponent evaluated from optical fiber fatigue data is distinctly lower (by about a factor of two [10-12]) than the corresponding parameter obtained from large-scale fracture specimens reinforce this conviction.

Our presentation will be made in two major parts. First, we shall summarize the results of some recent observations made on the kinetics of radial crack initiation in soda lime glass. It will be seen, from scanning electron micrographs of the indentations, that shear faults within the deformation zone act as the initiation precursors for the radial cracks. The threshold for pop-in is found to be highly sensitive to the contact period and to the presence of water. Fatigue data on the specimens indented at different loads, embracing the threshold, will then be presented. These data are interpreted in terms of initiation kinetics. The relevance of the interpretations to the mechanical behavior of optical fibers will remain an underlying motivation for the study.

Initiation Kinetics of Indentation Cracks

Microscopy of Flaws

In this section we discuss what we know about the nature of indentation flaws near the threshold load, as revealed by direct microscopical observa-

tions. The broader features of the typical deformation/fracture pattern, shown schematically in Fig. 1 for the Vickers indentation geometry, are readily discerned by conventional optical techniques; the scale of the flaw at radial crack pop-in is generally on the order $10\ \mu\text{m}$ for glass. It is this amenability to optical observation that has led to the relatively advanced state of our understanding of flaw response in the postthreshold region [1].

To understand the response in the subthreshold region, however, it becomes necessary to focus attention on events *within* rather than *without* the deformation zone. For this purpose one must go to higher resolution techniques, such as scanning electron microscopy. Figures 2 and 3 are appropriate photomicrographs of indentations in soda lime glass. In the first of these figures we see two simple top views of the same, postthreshold indentation before and after etching in dilute hydrofluoric acid. The etching reveals the detailed structure of the hardness impression more clearly, although one must be careful here in drawing conclusions about the immediate postindentation configuration; it is apparent from a comparison of Fig. 2*a* and *b* that the acid treatment has caused additional pop-in events to occur at the indentation corners, under the action of the residual stress field [13]. In Fig. 3 we see both top and side views (obtained by positioning the Vickers pyramid across a preexisting hairline crack and then running this crack through the specimen [6]) of a subthreshold indentation. Again, there is evidence of considerable fine structure in the deformation zone, particularly in the subsurface section.

The features of greatest interest in the scanning electron micrographs are the well-defined "fault" traces on the free surface areas which define the irreversible deformation zone. These faults appear from their geometry to be shear activated, much the same as classic dislocation slip processes in crystalline materials, although they operate at stress levels close to the theoretical limit of cohesive strength. One may conceive of the faulting configurations in terms of an intermittent "punching" mode, whereby catastrophic slip takes place at periodic intervals along shear stress trajectories to accommodate the intense strains exerted by the penetrating indenter [6]. For further geometri-

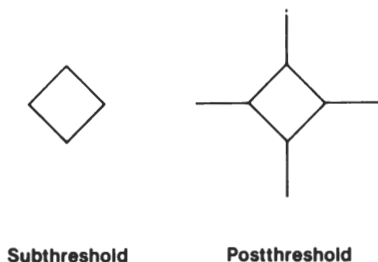


FIG. 1—Schematic of Vickers indentation geometry. Cracks pop in spontaneously at the threshold to the well-developed radial configuration.

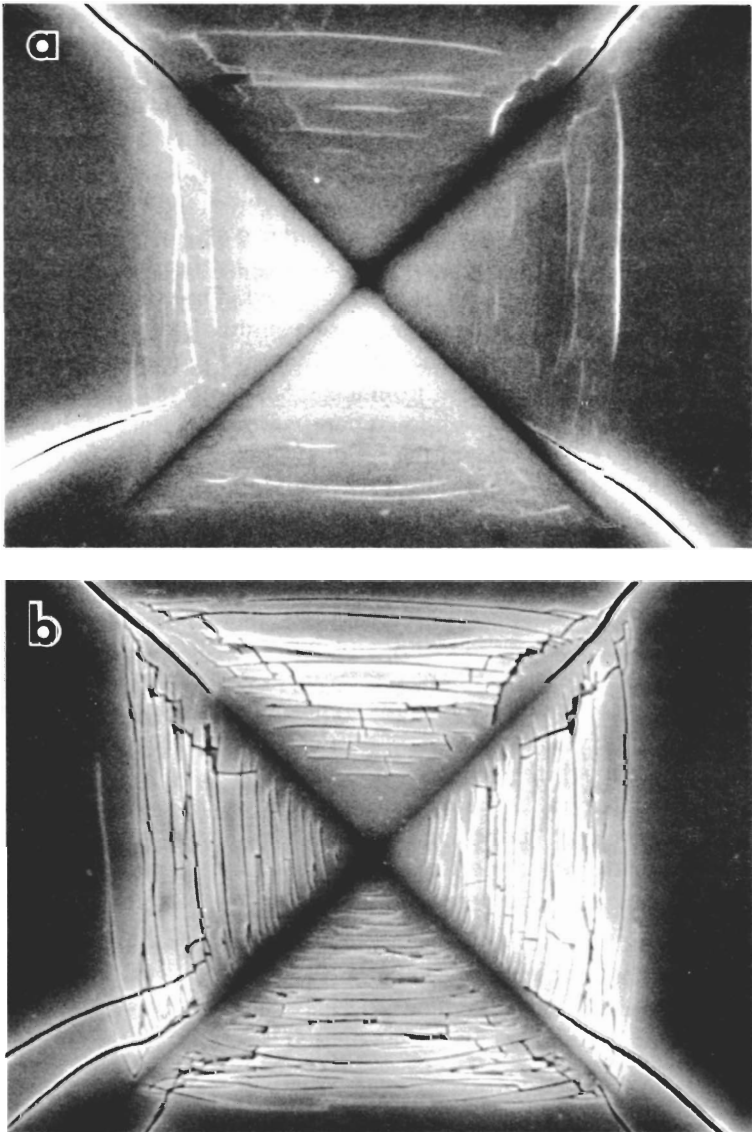


FIG. 2—Scanning electron micrographs of Vickers indentation in soda lime glass. Top views: (a) unetched and (b) etched. The indentation load is 4 N; width of field is 40 μm . Radial cracks initiate from the shear fault structure in the hardness zone.

cal details of the fault patterns, reference is made to the important papers by Hagan and Swain [14,15] on the subject.

The pertinent conclusions that we derive from the study of the micrographic evidence are as follows [6]:

1. The freshly created fault walls tend to recontact due to strongly compressive normal stresses within the contact zone, and thence to heal at the interface [6]. This healing is, nevertheless, incomplete since the faults remain susceptible to preferential etching.

2. Faults generated in different quadrants of the contact area can intersect to produce high stress intensifications (notwithstanding a certain ability for the faults to interpenetrate [15]), thus providing favorable sites for crack nucleation and growth.

3. The tendency for fault production to be intermittent (possibly because of the availability of suitable defect centers for the initial generation) leads to a certain variation in the geometrical disposition of the pattern from indentation to indentation (and even from quadrant to quadrant), thus giving rise to an element of scatter in the distribution of crack nuclei.

Kinetics of Crack Pop-In

It was indicated in the preceding subsection that optical techniques, although of insufficient resolution to observe the finer details of the precursor initiation processes, are usually adequate for observing the actual pop-in event itself. Here we describe the results of such observations made *in situ* through a microscope objective located immediately below the indentation site [6]. In our setup, a sinusoidal load-time pulse is applied to the Vickers indenter, and the time for radial pop-in, t_c , after the start of contact is recorded in relation to the indentation period, T . The functional interdependence of these two time variables then characterizes the kinetic response of the indentation flaws.

Typical results are shown in Fig. 4 for soda lime glass tested in air at a prescribed maximum load, P . It is immediately clear that the threshold condition is rate sensitive. At long contact periods pop-in occurs *during* the indentation cycle, specifically at a reproducible point $0.3 P$ on the unload half cycle. At short contact periods, however, pop-in occurs *after* the contact, generally with extensive delays, $t_c \gg T$, and with large scatter. These results show that the driving force for initiation is greatest while the indenter is under load but is nevertheless far from insignificant in the residual field. One may interpret the transition from short-contact to long-contact behavior in terms of an *incubation* time for development of a critical nucleus from the shear fault configuration. This incubation time is found to diminish as the peak contact load or the water content of the environment increases [6], consistent with the general fatigue experience.

Observations of this type lead us to the following picture of initiation kinet-

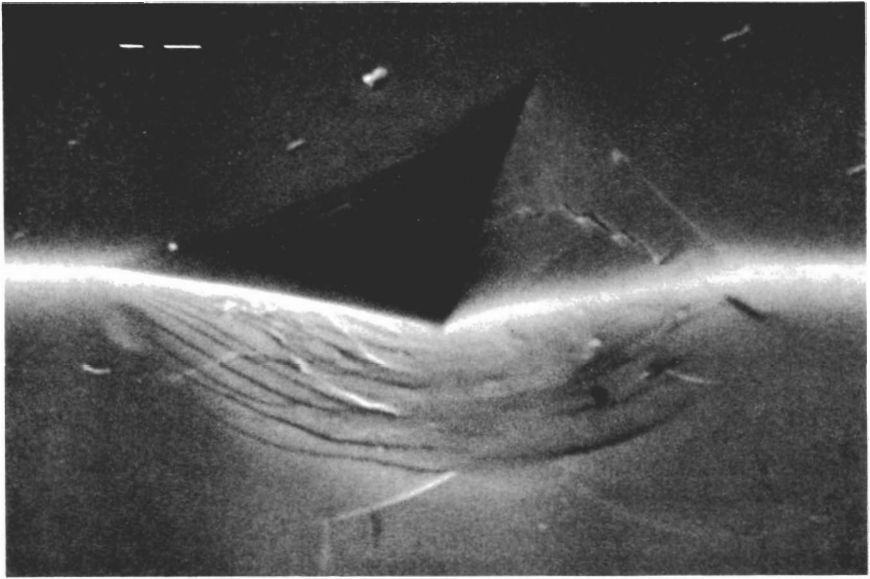


FIG. 3—Scanning electron micrograph of Vickers indentations in soda lime glass. Simultaneous top and side view. The indentation load is 1 N; width of field is 25 μm . Shear faults are evident below the hardness impression.

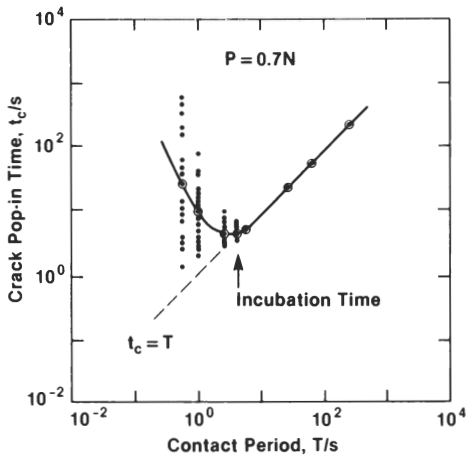


FIG. 4—Time to fracture as a function of the contact period for soda lime glass in air. The open symbols denote median values at each prescribed contact period. The results indicate an incubation time for development of a critical crack nucleus.

ics, based on the two-step process of precursor shear faulting and subsequent tensile crack pop-in [6]:

1. Newly formed shear faults become exposed to moisture in the environment, which penetrates into the interfaces and reduces the (already incomplete) cohesion. The penetration and decohesion mechanisms are both rate dependent, and therefore have the potential for controlling the kinetics. As this stage progresses, the stress intensifications at mutual fault intersection points increase, thereby building up the driving forces on the crack nuclei centers. It can be shown that the shear stress component responsible for activating the fault mechanisms reaches its maximum at the peak of indenter penetration but remains in force, albeit at reduced intensity, after completion of the cycle, consistent with the observations in Fig. 4.

2. The crack nuclei form close to the specimen surface, and are therefore similarly exposed to environmental moisture. Thus, unless the stress conditions are such that the nuclei propagate spontaneously to the fully developed radial configuration, the system will be subject to slow crack growth. The normal stresses on such nuclei remain compressive through most of the indentation cycle, becoming tensile only at the $0.3 P$ unload point. If the incubation time has been exceeded by the time this point is reached the critical nucleus, released of its constraint, becomes free to propagate immediately; if not, the incubation process continues in the weakened, residual stress field, in which case the pop-in kinetics become subject to the variability in nucleation centers alluded to earlier.

According to this description, either of these two steps could control the rate at which the critical stress intensification develops at the initiation center. Further work is needed to establish the relative importance of the shear fault and tensile crack concepts in the initiation kinetics.

Fatigue of Glass with Postthreshold and Subthreshold Indentation Flaws

We now examine the results of dynamic fatigue studies of soda lime glass containing postthreshold [4] and subthreshold [5] flaws. These studies were carried out using annealed rod specimens of 4 to 5-mm diameter, the surfaces of which had been preetched to remove large handling flaws and had been coated with protective lacquer over all but a central region ≈ 3 mm wide. Vickers indentations were placed in these uncoated test areas at prescribed peak loads, and were examined after 30 min to determine whether radial cracks had or had not popped in. The specimens were then stressed at constant rates in four-point flexure in water, with the indentation oriented for maximum tension, and their fatigue strengths duly recorded. In each case the broken specimens were checked to confirm that the failures had indeed originated from the indentation site; those that had not were omitted from the data accumulation.

Figure 5 shows the results for both postthreshold and subthreshold flaws, plotted in accordance with the master map scheme advocated in Ref 1. We recall from this earlier source that, for indentations with well-developed cracks, the dynamic fatigue response for any given material may be represented by the expression

$$\sigma_f P^{1/3} = (\lambda'_p \dot{\sigma}_a P)^{1/(n'+1)} \quad (1)$$

where P is the indentation load, $\dot{\sigma}_a$ is the stressing rate, σ_f is the strength, and n' and λ'_p are adjustable parameters. Both n' and λ'_p are load independent, so plotting in the coordinates of Fig. 5 should reduce all the data to a universal curve, regardless of the scale of the flaws. It is clear that there is a breakdown in this universality as one traverses the threshold into the low-load region:

1. The strengths are substantially higher, by a factor of three to four, consistent with the earlier study on fibers [7].
2. The scatter in data is wider, in correlation with the element of variability observed in the initiation kinetics (Fig. 4).
3. The susceptibility to fatigue is stronger; compare the apparent crack velocity exponents $n' = 9.0 \pm 0.8$ for subthreshold and $n' = 14.0 \pm 0.3$ for postthreshold.

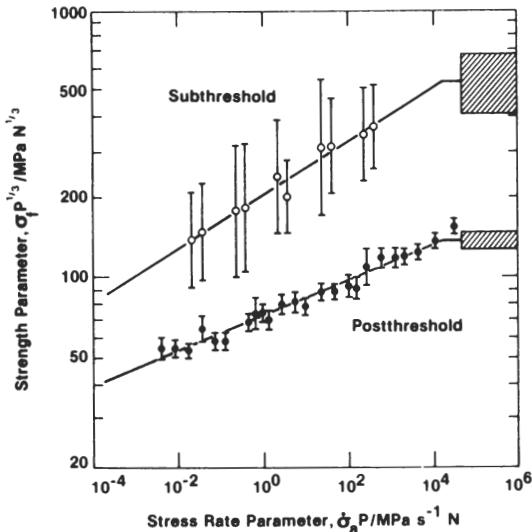


FIG. 5—Reduced dynamic fatigue plot for soda lime glass rods containing Vickers indentation flaws tested in water. The shaded bands indicate inert strength levels; the error bars are standard deviations; load range for postthreshold data is 0.05 to 10 N (see Ref 1) and for subthreshold data, 0.15 to 0.25 N.

Equation 1 is derived on the basis of specific assumptions concerning the flaw configuration, notably that the critical crack extension occurs in the far field of the initiation zone [1]. Therefore, it should not be altogether surprising that the subthreshold data plot onto a different curve in Fig. 5. The characteristics of the data in the two regions are, nevertheless, sufficiently diverse to suggest that we are dealing with two entirely different failure mechanisms, corresponding to a transition from propagation- to initiation-controlled instabilities. In this context it may be noted that the inert strength level for post-threshold flaws lies below the fatigue strength for subthreshold flaws over a large portion of the stressing rate range; thus, when radial cracks do initiate during a fatigue test, failure must occur spontaneously from the precursor shear fault configuration.

It is useful to replot the data in Fig. 5 in a way which brings out the scale effect more clearly. This is done in Fig. 6. To obtain this plot we have made use of the lifetime analogue of Eq 1 [1]; that is, substituting $\dot{\sigma}_a = \sigma_f/t_f$ and identifying σ_f with the constant applied stress σ_A , rearranged thus

$$t_f \sigma_A^{n'} = \lambda_p' / P^{(n'-2)/3} \quad (2)$$

as an explicit function of load. Each point in Fig. 6 accordingly represents a composite evaluation of $t_f \sigma_A^{n'}$ from all data at a given P , taking the two regions separately but using n' from the *postthreshold* curve fit in Fig. 5 as an appropriate fatigue exponent. The rationale for this choice of a common exponent is that, as mentioned before, the derivation of Eqs 1 and 2 is based strictly on the assumption that failure occurs from well-developed cracks. Thus, flaws which violate this assumption would be expected to show systematic departures from the baseline data curve, and this is indeed observed to be the case in Fig. 6. The solid line in this figure is equivalent to the prediction we would make using macroscopic crack laws (with due account of residual stress terms [1]); it is seen that such a prediction, extrapolated into the subthreshold domain, underestimates the lifetime at a fixed level of applied stress by several orders of magnitude.

It is useful to view the threshold phenomenon in Fig. 6 in terms of flaw size rather than indentation load. We have, accordingly, included a scale of the hardness impression a on the abscissa, using the hardness relation $H = P/2a^2 = 5.5$ GPa for Vickers indentations on glass as the basis for conversion. In the present case the threshold occurs in the range $a = 1$ to $10 \mu\text{m}$, although it must be remembered that this range can scale up or down, depending on the kinetic history of the flaw. The overlap between the subthreshold and postthreshold data is attributable to the variability in the shear fault configurations discussed earlier. Thus, it is conceivable that a particular flaw could be substantially smaller in its characteristic dimension than many of its possible competitors in a given specimen, and yet still control the strength properties by virtue of some uniquely favorable crack initiation conditions. Of

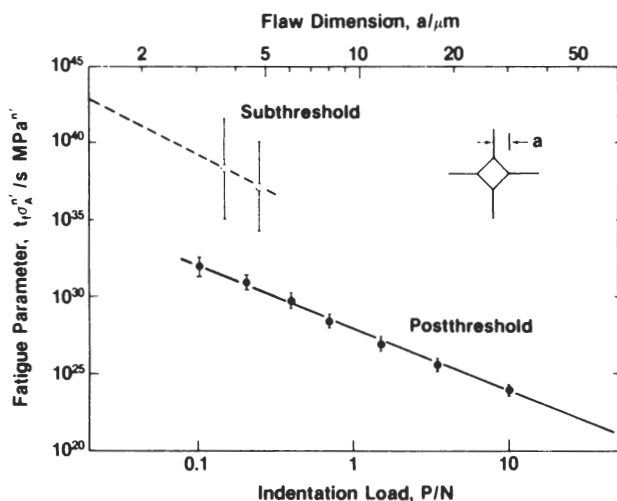


FIG. 6—Fatigue data from Fig. 5, replotted to show load (or equivalent flaw size) dependence. The error bars are standard deviations.

course, the potential always remains in such instances for delayed pop-in from some of these larger flaw centers, with consequent degradation in the overall lifetime response.

Implications Concerning Optical Fibers

We conclude this discourse by examining the implications of the results on the fatigue properties of ultrastrong silica fibers. The data presented here were obtained on rod rather than fiber specimens, and on soda lime rather than high silica glass. Although we have taken precautions to eliminate pre-existing handling flaws on our rod specimens, we can never be certain that the pristine surfaces of freshly drawn fibers would have responded in exactly the same way, and it is now well known that soda lime and high silica glasses differ significantly in their indentation behavior [16], the latter being regarded as anomalous in this respect. Nevertheless, it may be recalled that our very first observations of threshold effects in the strength behavior were on actual optical fibers [7], so we may feel justified in making certain predictions, if only of a qualitative nature.

One point that comes out clearly in the present work is the need to identify the flaw region which characterizes the operating stress range for a given component. Thus, if we wished to use the type of glass represented by the data in Figs. 5 and 6 as a structural material at ultrahigh strengths, it would hardly be efficient to design on the basis of extrapolations from the macroscopic crack region. (On the other hand, such extrapolations, in this case at least,

would suffice in applications calling for extreme conservatism in lifetime predictions.) These comments would appear to reinforce the conviction held by many that, as far as practically possible, design evaluations should be made using data taken on surfaces which have the same finish as those to be placed in service and which embrace the required lifetime. This is particularly so when adopting empirical approaches to flaw characterization, especially those based on statistical distribution functions, where the underlying processes responsible for creating the flaws in the first place are disregarded.

The point just made about designing within the time range of the fatigue data bears further elaboration here, for, as we have seen, flaws can continue to evolve long after their inception. Accordingly, where it is necessary to make extended lifetime predictions from relatively short-term fatigue data, the possibility exists for premature failures. Any amount of fatigue testing of control samples, or proof testing of actual components, will count for nothing if surfaces with subthreshold flaws are subsequently exposed to service environments conducive to crack initiation. There is some evidence from the glass fiber literature [17,18] that small-scale *natural* flaws can indeed suffer abrupt increases in severity with prolonged exposure to water, although in these cases direct observations of the flaws themselves could not be made to establish the nature of the transition. There would, accordingly, seem to be a strong case for advocating more controlled studies of fatigue failure in optical fibers, using flaws introduced by indentation or other artificial means, so that the fundamental lifetime-controlling processes might ultimately be identified and studied in a more systematic manner.

Acknowledgments

The authors gratefully acknowledge many useful discussions with R. F. Cook. Funding was provided by the U.S. Office of Naval Research (Metallurgy and Ceramics Program).

References

- [1] Cook, R. F. and Lawn, B. R., in this publication, pp. 22-42.
- [2] Lawn, B. R., *Journal of the American Ceramic Society*, Vol. 66, 1983, pp. 85-91.
- [3] Jakus, K., Ritter, J. E., and Babinski, R. C., in this publication, pp. 131-141.
- [4] Dabbs, T. P., Lawn, B. R., and Kelly, P. L., *Physics and Chemistry of Glasses*, Vol. 23, 1982, pp. 58-66.
- [5] Dabbs, T. P. and Lawn, B. R., *Physics and Chemistry of Glasses*, Vol. 23, 1982, pp. 93-97.
- [6] Lawn, B. R., Dabbs, T. P., and Fairbanks, C. J., *Journal of Materials Science*, Vol. 18, 1983, pp. 2785-2797.
- [7] Dabbs, T. P., Marshall, D. B., and Lawn, B. R., *Journal of the American Ceramic Society*, Vol. 63, 1980, pp. 224-225.
- [8] Lawn, B. R. and Evans, A. G., *Journal of Materials Science*, Vol. 12, 1977, pp. 2195-2199.
- [9] Lawn, B. R. and Marshall, D. B., *Journal of the American Ceramic Society*, Vol. 62, 1979, pp. 347-350.
- [10] Ritter, J. E. and Jakus, K., *Journal of the American Ceramic Society*, Vol. 60, 1977, p. 171.

- [11] Kalish, D. and Tariyal, B. K., *Journal of the American Ceramic Society*, Vol. 61, 1978, pp. 518-523.
- [12] Gulati, S. T., Helfinstine, J. D., Justice, B., McCartney, J. S., and Runyan, M. A., *American Ceramic Society Bulletin*, Vol. 58, 1979, pp. 1115-1117.
- [13] Dabbs, T. P. and Lawn, B. R., *Journal of the American Ceramic Society*, Vol. 65, 1982, pp. C37-C38.
- [14] Hagan, J. T. and Swain, M. V., *Journal of Physics D: Applied Physics*, Vol. 11, 1978, pp. 2091-2102.
- [15] Hagan, J. T., *Journal of Materials Science*, Vol. 15, 1980, pp. 1417-1424.
- [16] Arora, A., Marshall, D. B., Lawn, B. R., and Swain, M. V., *Journal of Non-Crystalline Solids*, Vol. 31, 1979, pp. 415-428.
- [17] Chandan, H. C. and Kalish, D., *Journal of the American Ceramic Society*, Vol. 65, 1982, pp. 171-173.
- [18] Gupta, P. K., in *Fracture Mechanics of Ceramics*, R. C. Bradt, A. G. Evans, D. P. H. Hasselman, and F. F. Lange, Eds., Plenum, New York, 1982, pp. 291-303.